

BAT AGN Spectroscopic Survey-III. An observed link between AGN Eddington ratio and narrow emission line ratios

Kyuseok Oh^{1*}, Kevin Schawinski¹, Michael Koss^{1,11}, Benny Trakhtenbrot^{1,12}, Isabella Lamperti¹, Claudio Ricci², Richard Mushotzky³, Sylvain Veilleux³, Simon Berney¹, D. Michael Crenshaw⁴, Neil Gehrels⁵, Fiona Harrison⁶, Nicola Masetti^{7,8}, Kurt T. Soto¹, Daniel Stern⁹, Ezequiel Treister², Yoshihiro Ueda¹⁰

¹*Institute for Astronomy, Department of Physics, ETH Zurich, Wolfgang-Pauli-Strasse 27, CH-8093 Zurich, Switzerland*

²*Instituto de Astrofísica, Facultad de Física, Pontificia Universidad Católica de Chile, Casilla 306, Santiago 22, Chile*

³*Astronomy Department and Joint Space-Science Institute, University of Maryland, College Park, MD, USA*

⁴*Department of Physics and Astronomy, Georgia State University, Astronomy Offices, One Park Place South SE, Suite 700, Atlanta, GA 30303, USA*

⁵*NASA Goddard Space Flight Center, Greenbelt, MD 20771, USA*

⁶*Cahill Center for Astronomy and Astrophysics, California Institute of Technology, Pasadena, CA 91125, USA*

⁷*INAF - Istituto di Astrofisica Spaziale e Fisica Cosmica di Bologna, via Gobetti 101, 40129 Bologna, Italy*

⁸*Departamento de Ciencias Físicas, Universidad Andrés Bello, Fernández Concha 700, Las Condes, Santiago, Chile*

⁹*Jet Propulsion Laboratory, California Institute of Technology, 4800 Oak Grove Drive, MS 169-224, Pasadena, CA 91109, USA*

¹⁰*Department of Astronomy, Kyoto University, Kyoto 606-8502, Japan*

¹¹*Ambizione fellow*

¹²*Zwicky fellow*

Accepted XXX. Received YYY; in original form ZZZ

ABSTRACT

We investigate the observed relationship between black hole mass (M_{BH}), bolometric luminosity (L_{bol}), and Eddington ratio (λ_{Edd}) with optical emission line ratios ([N II] $\lambda 6583/\text{H}\alpha$, [S II] $\lambda\lambda 6716, 6731/\text{H}\alpha$, [O I] $\lambda 6300/\text{H}\alpha$, [O III] $\lambda 5007/\text{H}\beta$, [Ne III] $\lambda 3869/\text{H}\beta$, and He II $\lambda 4686/\text{H}\beta$) of hard X-ray-selected AGN from the BAT AGN Spectroscopic Survey (BASS). We show that the [N II] $\lambda 6583/\text{H}\alpha$ ratio exhibits a significant correlation with λ_{Edd} ($R_{\text{Pear}} = -0.44$, $p\text{-value} = 3 \times 10^{-13}$, $\sigma = 0.28$ dex), and the correlation is not solely driven by M_{BH} or L_{bol} . The observed correlation between [N II] $\lambda 6583/\text{H}\alpha$ ratio and M_{BH} is stronger than the correlation with L_{bol} , but both are weaker than the λ_{Edd} correlation. This implies that the large-scale narrow lines of AGN host galaxies carry information about the accretion state of the AGN central engine. We propose that the [N II] $\lambda 6583/\text{H}\alpha$ is a useful indicator of Eddington ratio with 0.6 dex of rms scatter, and that it can be used to measure λ_{Edd} and thus M_{BH} from the measured L_{bol} , even for high redshift obscured AGN. We briefly discuss possible physical mechanisms behind this correlation, such as the mass-metallicity relation, X-ray heating, and radiatively driven outflows.

Key words: galaxies: active – galaxies: nuclei – quasars: general – black hole physics

1 INTRODUCTION

Nebular emission lines are a powerful tool for diagnosing the physical state of ionized gas and studying central nuclear activity. Optical emission line ratios can be used to discriminate between emission from the star formation in galaxies and harder radiation such as from

the central nuclear activity around a supermassive black holes (e.g., Baldwin et al. 1981; Veilleux & Osterbrock 1987; Kewley et al. 2001; Kauffmann et al. 2003). Compared to star forming galaxies, active galactic nuclei (AGN) produce greater numbers of higher energy photons (e.g., UV and X-rays) and, therefore drive higher ratios of the collisionally excited forbidden lines compared to the photoionization-induced Balmer emission lines. Although such line ratios provide useful AGN diagnostics, even for obscured AGN

* E-mail: ohk@phys.ethz.ch

(Reyes et al. 2008; Yuan et al. 2016), they may not be effective in selecting all heavily obscured AGN and/or AGN that lack significant amounts of low density gas (Elvis et al. 1981; Iwasawa et al. 1993; Griffiths et al. 1995; Barger et al. 2001; Comastri et al. 2002; Rigby et al. 2006; Caccianiga et al. 2007).

With the recent advent of hard X-ray (> 10 keV) facilities, such as *INTEGRAL* (Winkler et al. 2003), *Swift* (Gehrels et al. 2004) and *NuSTAR* (Harrison et al. 2013), it is now possible to study samples of AGN that are less biased to obscuration and include even Compton thick sources ($N_{\text{H}} > 10^{24} \text{ cm}^{-2}$, Ricci et al. 2015; Koss et al. 2016). In particular, the Burst Alert Telescope (BAT, Barthelmy et al. 2005) on board the *Swift* satellite has been observing the sky in the 14–195 keV energy band since 2005, reaching sensitivities of $1.3 \times 10^{-11} \text{ erg cm}^{-2} \text{ s}^{-1}$ over 90% of the sky. The 70 month *Swift*-BAT all-sky hard X-ray survey¹ detected 1210 objects, of which 836 are AGN (Baumgartner et al. 2013). While the BAT detection is relatively unabsorbed up to Compton thick levels (e.g., $N_{\text{H}} < 10^{24} \text{ cm}^{-2}$, Koss et al. 2016) heavily Compton thick AGN ($N_{\text{H}} > 10^{25} \text{ cm}^{-2}$) are missed by X-ray surveys but may sometimes be detected using optical emission line diagnostics and strong [O III] $\lambda 5007$ emission lines (e.g., Maiolino et al. 1998).

The relationship between Eddington ratio ($\lambda_{\text{Edd}} \equiv L/L_{\text{Edd}}$, where $L_{\text{Edd}} \equiv 1.3 \times 10^{38} M_{\text{BH}}/M_{\odot}$) and the position of AGN in emission-line diagrams is an important topic of study because of the difficulty in measuring black hole mass (M_{BH}) from velocity dispersion in high redshift AGN. Kewley et al. (2006) investigated host properties of nearby emission-line galaxies ($0.04 < z < 0.1$) from the SDSS. They found that the λ_{Edd} (inferred from $L_{[\text{O III}]}/\sigma_{*}^4$, where σ_{*} is a stellar velocity dispersion) shows an increase with ϕ , a measure of distance from the LINER regime in the [O III] $\lambda 5007/\text{H}\beta$ vs. [O I] $\lambda 6300/\text{H}\alpha$ diagram. Similarly, an SDSS study of unobscured AGN by Stern & Laor (2013) found a dependence of emission-line diagnostics on the λ_{Edd} . However, the estimation of λ_{Edd} and the introduced relationship between the angle ϕ and $L_{[\text{O III}]}/\sigma_{*}^4$ were both dependent on the strength of [O III] $\lambda 5007$. Also, the previous studies did not take into account X-ray selection focusing on the large sample of optically selected AGN. Both highly ionized optical emission lines and X-rays are thought to be a measure of the AGN bolometric luminosity. However, hard X-rays are less biased against dust obscuration and the contribution from star-forming activity than optical emission lines.

The BAT AGN Spectroscopic Survey (BASS) Data Release 1 (Koss et al., in submitted) compiled 642 optical spectra of nearby AGN ($\langle z \rangle \sim 0.05$) from public surveys (SDSS, 6dF; Abazajian et al. 2009; Jones et al. 2009; Alam et al. 2015) and dedicated follow-up observations (e.g., from telescopes at the Kitt Peak, Gemini, Palomar, and SAAO observatories). The data release provided emission line measurements as well as M_{BH} and λ_{Edd} estimates for the majority of obscured and un-obscured AGN (74%, 473/642), including 340 AGN with M_{BH} measurements reported for the first time.

In this paper, we use the BASS measurements to in-

vestigate the observed relationship between black hole mass (M_{BH}), bolometric luminosity (L_{bol}), and Eddington ratio (λ_{Edd}) with optical emission line ratios ([N II] $\lambda 6583/\text{H}\alpha$, [S II] $\lambda \lambda 6716, 6731/\text{H}\alpha$, [O I] $\lambda 6300/\text{H}\alpha$, [O III] $\lambda 5007/\text{H}\beta$, [Ne III] $\lambda 3869/\text{H}\beta$, and He II $\lambda 4686/\text{H}\beta$) for both obscured and unobscured AGN.

We assume a cosmology with $h = 0.70$, $\Omega_{\text{M}} = 0.30$, and $\Omega_{\Lambda} = 0.70$ throughout this work.

2 SAMPLE SELECTION, DATA, AND MEASUREMENTS

In this section, we briefly summarize the measurement procedures for optical emission lines, M_{BH} , and λ_{Edd} . The BASS DR1 measured nebular emission line strengths by performing a power-law fit with Gaussian components to model the continuum and emission lines. For unobscured AGN, two Gaussian components are allowed in the H α and H β emission line regions to account for both broad (FWHM $> 1000 \text{ km s}^{-1}$) and narrow (FWHM $< 1000 \text{ km s}^{-1}$) components. When broad H β is detected, M_{BH} is measured using the single-epoch method following Trakhtenbrot & Netzer (2012). If no broad H β is detected, M_{BH} is measured based on the line width and luminosity of broad H α (equation 9 from Greene & Ho 2005). For obscured AGN, the estimation of M_{BH} relies on the close correlations between M_{BH} and the stellar velocity dispersion (σ_{*} , e.g., Kormendy & Ho 2013). Stellar velocity dispersion is derived from the penalised pixel fitting method (pPXF, Cappellari & Emsellem 2004) by implementing a modified version of the masking procedure introduced for the analysis of SDSS DR7 (Abazajian et al. 2009) galaxy spectra (the OSSY catalog², Sarzi et al. 2006; Oh et al. 2011, 2015).

Since the obscuration mostly affect the estimation of L_{bol} for Compton thick AGN ($N_{\text{H}} > 10^{24} \text{ cm}^{-2}$), we estimated L_{bol} from the intrinsic (i.e., absorption and k-corrected) 14–150 keV luminosities reported in Ricci et al. (2015) and Ricci et al. (in prep.), transforming them into 14–195 keV luminosities assuming a power-law continuum with a photon index of $\Gamma = 1.9$. After converting the 14–195 keV luminosity to the intrinsic 2–10 keV luminosity the procedure described by following Rigby et al. (2009), we then applied the median bolometric correction introduced by Vasudevan et al. (2009). It is noteworthy to mention that the estimation of L_{bol} comes solely from hard X-ray band (14–195 keV) and its constant conversion factor ($k = 8$). We briefly discuss the effect of different L_{bol} estimation in Section 3. We then combined the measured M_{BH} with the L_{bol} to calculate λ_{Edd} ($\lambda_{\text{Edd}} \equiv L_{\text{bol}}/L_{\text{Edd}}$) assuming $L_{\text{Edd}} \equiv 1.3 \times 10^{38} (M_{\text{BH}}/M_{\odot})$. For more details, refer to the first data release (Koss et al., in submitted).

We focus on the sub-sample of the 642 optical spectra from the BASS DR1. We consider only non-beamed AGN, which were selected by cross-matching the BASS sources with the Roma blazar catalog (BZCAT) v5.0 (Massaro et al. 2009). We then restricted our samples to redshifts of $0.01 < z < 0.40$ to have coverage of the H β and H α region. Berney et al. (2015) investigated the effect of slit size for the

¹ <http://heasarc.gsfc.nasa.gov/docs/swift/results/bs70mon/>

² <http://gem.yonsei.ac.kr/ossy/>

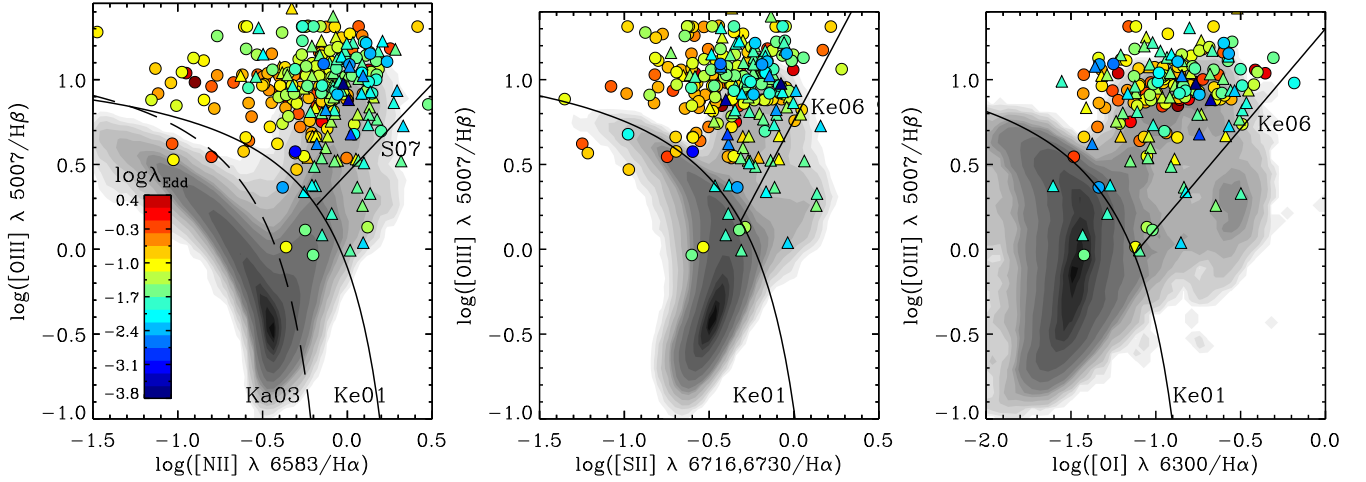


Figure 1. Emission line diagnostic diagrams for the BASS sources with signal-to-noise (S/N) ratio > 3 . Left: The $[\text{N II}] \lambda 6583/\text{H}\alpha$ versus $[\text{O III}] \lambda 5007/\text{H}\beta$ diagnostic diagram. Colour filled circles and triangles indicate type 1 AGNs (including type 1.9) and type 2 AGNs, respectively. The empirical star-formation curve obtained from [Kauffmann et al. \(2003\)](#) (dashed curve) and the theoretical maximum starburst model of [Kewley et al. \(2001\)](#) (solid curve) are used. The solid-straight line is the empirical demarcation of [Schawinski et al. \(2007\)](#) distinguishing the Seyfert AGN from the LINERs. The Eddington ratio of BASS sources is shown with color-filled dots. Middle: The $[\text{S II}] \lambda \lambda 6716, 6731/\text{H}\alpha$ versus $[\text{O III}] \lambda 5007/\text{H}\beta$ diagnostic diagram. Demarcation lines from [Kewley et al. \(2001, 2006\)](#) are used. In all panels we also show more than 180,000 SDSS emission-line galaxies with filled contours chosen from the OSSY catalog ($z < 0.2$) with $\text{S/N} > 3$ for $[\text{N II}] \lambda 6583$, $\text{H}\alpha$, $[\text{O III}] \lambda 5007$, $\text{H}\beta$, $[\text{S II}] \lambda 6716$, and $[\text{O I}] \lambda 6300$.

Table 1. Bayesian linear regression fit.

line ratio (1)	N (2)	α (3)	β (4)	RMSD (5)	R_{Pear} (p -value) (6)	$R_{\text{Pear,unobs}}$ (p -value) (7)	$R_{\text{Pear,obs}}$ (p -value) (8)
$[\text{N II}] \lambda 6583/\text{H}\alpha$	297	-0.42 ± 0.04	-0.19 ± 0.02	0.28	$-0.44 (3 \times 10^{-13})$	$-0.34 (0.00002)$	$-0.28 (0.00128)$
$[\text{S II}] \lambda \lambda 6716, 6731/\text{H}\alpha$	288	-0.48 ± 0.03	-0.11 ± 0.02	0.25	$-0.29 (9 \times 10^{-7})$	$-0.26 (0.00080)$	$0.11 (0.56180)$
$[\text{O I}] \lambda 6300/\text{H}\alpha$	205	(0.03314)	(0.02777)	(0.36499)
$[\text{O III}] \lambda 5007/\text{H}\beta$	286	(0.32877)	(0.38456)	(0.34875)
$[\text{Ne III}] \lambda 3869/\text{H}\beta$	125	(0.87141)	(0.38163)	(0.78629)
$\text{He II} \lambda 4686/\text{H}\beta$	107	(0.87516)	(0.56490)	(0.08583)

Note. (1) optical emission line ratio; (2) size of sample; (3) intercept; (4) slope; (5) rms deviation; (6) Pearson R coefficient and p -value; (7) Pearson R coefficient and p -value for unobscured AGN; (8) Pearson R coefficient and p -value for obscured AGN.

BASS DR1 sources and showed that the ratio between extinction corrected $L[\text{O III}]$ and $L_{14-195\text{keV}}$ is constant when excluding the nearest galaxies ($z < 0.01$) while the scatter slightly decreases towards larger slit sizes. We used the same redshift range following this approach. However, it should be noted that aperture effect does not change our results shown in Section 3. We tested whether sources with large physical coverage (> 2 kpc) still found a significant correlation in a smaller sample size suggesting that slit size is not important for this study. We also selected only spectral fits with a good quality as listed in the DR1 tables (Koss et al., in submitted). We note that sources with spectra taken from the 6dF Galaxy Survey ([Jones et al. 2009](#)) are only used to derive emission line ratios and to measure stellar velocity dispersions (e.g., [Campbell et al. 2014](#)) due to the lack of flux calibration as necessary for broad line black hole mass measurements. Samples sizes for each emission line ratio used in this paper are listed in Table 1.

3 RELATIONS BETWEEN OPTICAL EMISSION LINE RATIOS AND BASIC AGN PROPERTIES

Fig. 1 shows the emission-line diagnostic diagrams for the BASS sources according to λ_{Edd} (colour-coded). The majority of the BASS sources ($> 90\%$) are found in the Seyfert region in each panel.

In order to study the statistical significance of any correlations with λ_{Edd} , we show optical emission line ratios as a function of λ_{Edd} in Fig. 2. We performed Bayesian linear regression fit (equation 1) to all points using the method of [Kelly \(2007\)](#) which accounts for measurement errors in both axes. The relation between λ_{Edd} and optical emission line ratio (black solid line in Fig. 2) is determined by taking the median of 10,000 draws from the posterior probability distribution of the converged parameters (intercept and slope). The errors of intercept and slope are reported from

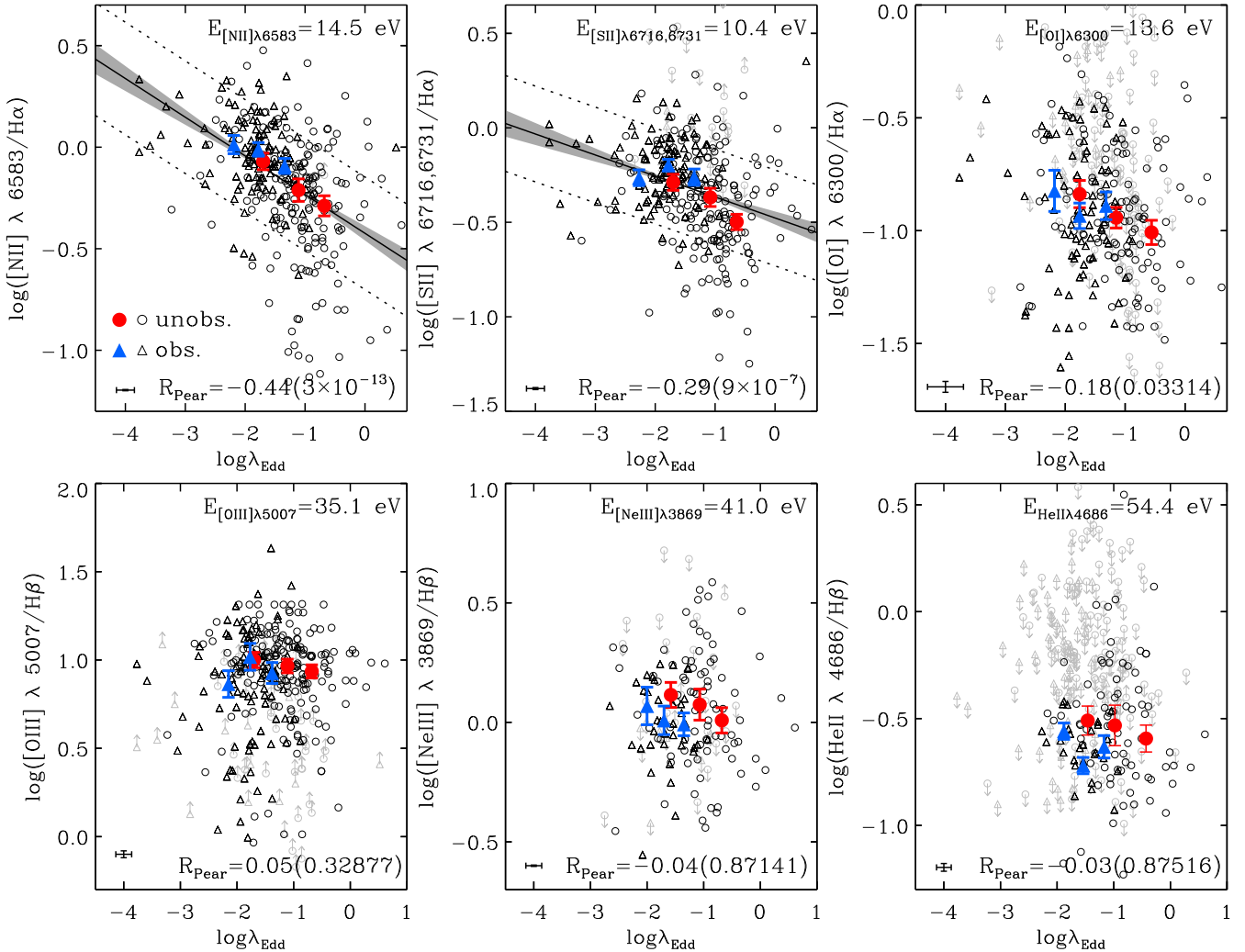


Figure 2. Optical emission line ratio versus Eddington ratio diagram. Black open circles and triangles indicate type 1 AGN (including type 1.9) and type 2 AGN, respectively. Median at each bin is shown with colour-filled symbols. Bin size is determined to have at least 10 sources. Black solid lines indicate the Eddington ratio - optical emission line relations (equation 1). The grey shaded regions account for the errors in the slope and intercept of the relation. The rms deviation is shown with dotted lines. An error bar in the bottom-left corner at each panel indicates typical uncertainties in Eddington ratio and optical emission line ratio. The ionization potential for each emission line is shown in the legends. Also, Pearson correlation coefficients and p -values are shown in the bottom-right corner of each panel. An emission line detection at $S/N < 3$ (upper- or lower-limit) is shown with grey symbols.

1σ confidence ellipse. The root-mean-square (rms) deviation is shown with black dotted lines at each panel.

$$\log(F_{\text{line}}/F_{\text{Balmer}}) = \alpha + \beta \log \lambda_{\text{Edd}} \quad (1)$$

The values of α (intercept), β (slope), Pearson correlation coefficient, rms deviation, and p -value are summarised in Table 1.

We find that the λ_{Edd} is significantly anti-correlated with optical emission line ratios for both the $[\text{N II}] \lambda 6583/\text{H}\alpha$ and $[\text{S II}] \lambda \lambda 6716, 6731/\text{H}\alpha$ ratios but not for the other line ratios. The larger the λ_{Edd} , the smaller the line ratio of $[\text{N II}] \lambda 6583/\text{H}\alpha$ and $[\text{S II}] \lambda \lambda 6716, 6731/\text{H}\alpha$. We find that Pearson R coefficient and p -value of the anti-correlation between $[\text{N II}] \lambda 6583/\text{H}\alpha$ and λ_{Edd} are -0.44 and 3×10^{-13} , respectively, with 0.28 dex of rms deviation. We also found a significantly anti-correlated relationship for both the $[\text{N II}] \lambda 6583/\text{H}\alpha$ and $[\text{S II}] \lambda \lambda 6716, 6731/\text{H}\alpha$

ratios with a more stringent S/N cut of optical emission lines (> 10). AGN variability may induces the scatter shown in the anti-correlation between $[\text{N II}] \lambda 6583/\text{H}\alpha$ and λ_{Edd} . Since X-ray emission that we used to derive L_{bol} and λ_{Edd} has different time-scales compared to optical narrow emission lines, a scatter around the anti-correlation can be explained (Mushotzky et al. 1993; Schawinski et al. 2015). Also, differences in metallicities and/or structures of the narrow-line regions may contribute to the scatter shown above. In order to quantitatively investigate if the λ_{Edd} shows a stronger anti-correlation with $[\text{N II}] \lambda 6583/\text{H}\alpha$ or with $[\text{S II}] \lambda \lambda 6716, 6731/\text{H}\alpha$, we run a z -test based on the two Pearson correlation coefficients (Fisher r -to- z transformation). The p -value (0.019) suggests that $[\text{N II}] \lambda 6583/\text{H}\alpha$ shows a significantly stronger anti-correlation than $[\text{S II}] \lambda \lambda 6716, 6731/\text{H}\alpha$ with λ_{Edd} .

Moreover, we also find that the observed anti-

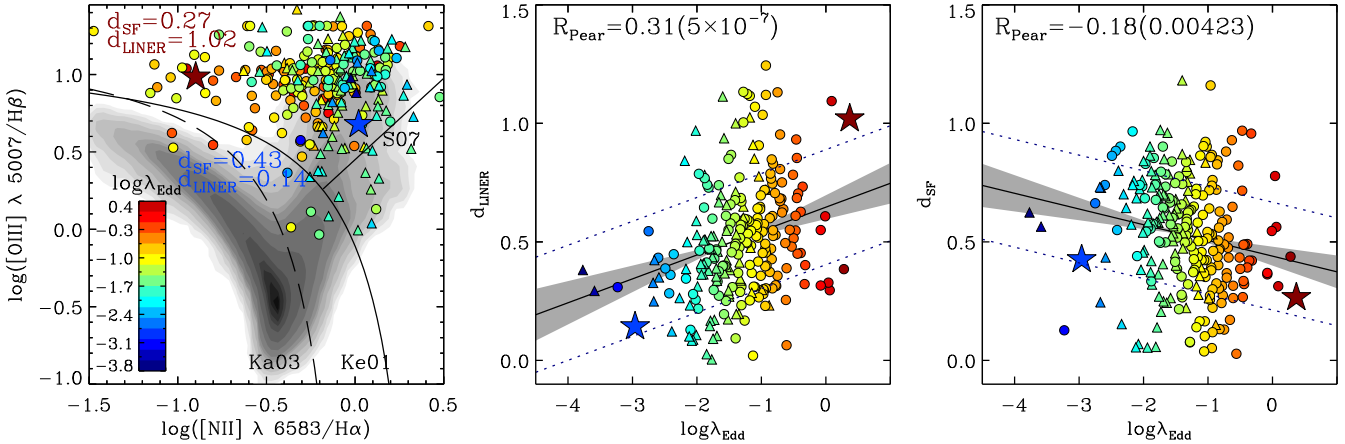


Figure 3. d_{LINER} and d_{SF} as a function of Eddington ratio. Left panel illustrates distances of two examples (star symbols) with corresponding color-coded Eddington ratio as in Fig. 1. Middle and right panels show the d_{LINER} and d_{SF} distributions, respectively. Bayesian linear regression fit, errors in the slope, intercept of the fit, and the rms deviation are shown with black straight lines, grey shaded regions and dotted lines, as in Fig. 2.

correlation between $[\text{N II}] \lambda 6583/\text{H}\alpha$ and λ_{Edd} is valid for obscured AGN (blue filled triangles in Fig. 2) as well as unobscured AGN (red filled circles in Fig. 2). Pearson R coefficient and p -value for obscured AGN are -0.28 and 0.00128 , respectively. For unobscured AGN, we report -0.34 and 0.00002 as Pearson R coefficient and p -value. We report that λ_{Edd} can be estimated from the measured $[\text{N II}] \lambda 6583/\text{H}\alpha$ ratio as follows, with 0.6 dex of rms deviation:

$$\log \lambda_{\text{Edd}} = (-1.52 \pm 0.04) + (-1.00 \pm 0.13) \times \log([\text{N II}] \lambda 6583/\text{H}\alpha) \quad (2)$$

Another way to study the location on the emission line diagnostic diagram is to measure the shortest distance from the star-forming and LINER lines in $[\text{N II}] \lambda 6583/\text{H}\alpha$. The λ_{Edd} distribution shown in the $[\text{N II}] \lambda 6583/\text{H}\alpha$ emission line diagnostic diagram (left panel of Fig. 1) enables us to infer that AGN falling in the Seyfert region exhibit different λ_{Edd} according to their location, i.e., combinations of emission line ratios. We define the distance between the location of a given object and the empirical demarcation line of Schawinski et al. (2007) (d_{LINER}) and the theoretical maximum starburst model of Kewley et al. (2001) (d_{SF}). The separation between Seyfert and LINER was obtained by visual determination based on $[\text{N II}] \lambda 6583/\text{H}\alpha$ vs. $[\text{O III}] \lambda 5007/\text{H}\beta$ diagram for nearly 50,000 nearby SDSS galaxies ($0.05 < z < 0.10$, Schawinski et al. 2007). For Seyfert and LINERs classified using the $[\text{S II}] \lambda \lambda 6716, 6731/\text{H}\alpha$ and $[\text{O I}] \lambda 6300/\text{H}\alpha$ diagrams, the authors determined the demarcation line in the $[\text{N II}] \lambda 6583/\text{H}\alpha$ diagram. In particular, we measured d_{SF} by moving the demarcation line of Kewley et al. (2001) in parallel with the original one until it matches the location of the given object. The measured distance, d_{LINER} , that originated from optical emission line ratios which depict the physical state of the innermost region of the galaxy is a function of the λ_{Edd} (middle panel in Fig. 3). We report Pearson R coefficient and p -value for d_{LINER} and $\log \lambda_{\text{Edd}}$ with 0.31 and 5×10^{-7} while d_{SF} shows less significant statistics ($R_{\text{Pear}} = -0.18$, p -value = 0.00423) suggesting that λ_{Edd} is less likely a function of d_{SF} . We also ran a test to see if sources with extreme λ_{Edd} were driving correlations

we found. For this test, we used a limited range of λ_{Edd} ($-2.67 < \log \lambda_{\text{Edd}} < 0.00$) which excludes small number of objects shown at both high- and low-end of λ_{Edd} and we found a significant correlation.

We further study the observed anti-correlation by looking for correlations with M_{BH} (Fig. 4). We find that the $[\text{N II}] \lambda 6583/\text{H}\alpha$, $[\text{S II}] \lambda \lambda 6716, 6731/\text{H}\alpha$, $[\text{O I}] \lambda 6300/\text{H}\alpha$, and $[\text{O III}] \lambda 5007/\text{H}\beta$ show positive correlations with M_{BH} , with p -values of 5×10^{-6} , 0.00218, 0.00009, and 0.00174, respectively. In order to understand whether the anti-correlation of $[\text{N II}] \lambda 6583/\text{H}\alpha$ with λ_{Edd} is stronger than the correlation of $[\text{N II}] \lambda 6583/\text{H}\alpha$ with M_{BH} we run the z -test based on the two Pearson correlation coefficients and find that the p -value suggests a stronger anti-correlation for the λ_{Edd} (p -value = 0.025). We also investigate the observed anti-correlation between optical emission line ratios and λ_{Edd} with fixed M_{BH} ($7 < \log(M_{\text{BH}}/M_{\odot}) < 8$, $8 < \log(M_{\text{BH}}/M_{\odot}) < 9$). We find that $[\text{N II}] \lambda 6583/\text{H}\alpha$ is indeed significantly anti-correlated with λ_{Edd} in each of these mass bins, with p -value of 0.00488 ($7 < \log(M_{\text{BH}}/M_{\odot}) < 8$) and 3×10^{-7} ($8 < \log(M_{\text{BH}}/M_{\odot}) < 9$). On the other hand, the other line ratios do not show correlation with λ_{Edd} at any fixed M_{BH} except $[\text{S II}] \lambda \lambda 6716, 6731/\text{H}\alpha$ which shows p -value of 5×10^{-5} in high M_{BH} bin. We also test how the relationships between emission line ratios and M_{BH} change at fixed λ_{Edd} ($-2.5 < \log \lambda_{\text{Edd}} < -1.5$, $-1.5 < \log \lambda_{\text{Edd}} < -0.5$). We find that $[\text{O I}] \lambda 6300/\text{H}\alpha$ and $[\text{O III}] \lambda 5007/\text{H}\beta$ only show weak correlation at both fixed λ_{Edd} bins with less than 1% level of p -value.

Finally, we find a negative correlation with the L_{bol} (Fig. 5) for $[\text{N II}] \lambda 6583/\text{H}\alpha$ (p -value = 0.00577) while a positive correlation is found for $[\text{O III}] \lambda 5007/\text{H}\beta$ (p -value = 2×10^{-6}). Running the z -test based on the two Pearson correlation coefficients for $[\text{N II}] \lambda 6583/\text{H}\alpha$ with λ_{Edd} compared to $[\text{N II}] \lambda 6583/\text{H}\alpha$ with L_{bol} again suggests a statistically stronger correlation (p -value = 0.0001) in λ_{Edd} . While $[\text{N II}] \lambda 6583/\text{H}\alpha$ shows correlations with M_{BH} and L_{bol} , the correlation with M_{BH} is more significant at the less than 5% level based on a Fisher z test (p -value = 0.036).

In order to understand effect of the different bolo-

metric correction, we estimate L_{bol} and λ_{Edd} following Marconi et al. (2004) who uses bolometric correction that depends on 2-10 keV luminosity (equation 21 in their paper). The mean difference between the newly estimated L_{bol} and the one derived by our prescription is 0.03 dex with 0.33 dex of scatter, which gives a mean difference in λ_{Edd} of 0.03 dex (0.33 dex of scatter). We find that [N II] $\lambda 6583/\text{H}\alpha$ (p -value= 10^{-12}) and [S II] $\lambda\lambda 6716, 6731/\text{H}\alpha$ (p -value= 1×10^{-6}) show significant anti-correlation with λ_{Edd} .

If we adopt more steep bolometric correction curve that varies with 2-10 keV luminosity (see Figure 3 in Marconi et al. 2004) covering wide range of bolometric correction, we may get flattened relationship in [N II] $\lambda 6583/\text{H}\alpha$ and λ_{Edd} as sources in low λ_{Edd} and high λ_{Edd} move toward each end. However, we find that the application of such extreme case of bolometric correction does not significantly change the Pearson R coefficient (-0.43) and p -value (10^{-12}) but shows slightly moderate slope (-0.10 ± 0.01).

4 DISCUSSION

We have presented the observed relationship between the λ_{Edd} and optical emission line ratios ([N II] $\lambda 6583/\text{H}\alpha$, [S II] $\lambda\lambda 6716, 6731/\text{H}\alpha$, [O I] $\lambda 6300/\text{H}\alpha$, [O III] $\lambda 5007/\text{H}\beta$, [Ne III] $\lambda 3869/\text{H}\beta$, and He II $\lambda 4686/\text{H}\beta$) using local obscured and unobscured AGN ($\langle z \rangle = 0.05$, $z < 0.40$) from the 70-month *Swift*-BAT all-sky hard X-ray survey with follow-up optical spectroscopy. We show that there is a significant anti-correlation between [N II] $\lambda 6583/\text{H}\alpha$ emission line ratio and λ_{Edd} , and this correlation is stronger than trends with M_{BH} or L_{bol} or with other line ratios. The observed trend suggests that optical emission line ratios, which are widely used to classify sources as AGN, can also be an indicator of λ_{Edd} . The use of [N II] $\lambda 6583$ and $\text{H}\alpha$ emission lines as a λ_{Edd} indicator has potential implications for high redshift obscured AGN whose M_{BH} and λ_{Edd} are difficult to estimate. This would require to additionally assume that any relevant physical relations that might affect our λ_{Edd} - [N II] $\lambda 6583/\text{H}\alpha$ relation (e.g., the stellar mass-metallicity, AGN outflows), do not evolve significantly with redshift. The relationship shown in this work may serve as a basis for future studies toward measuring M_{BH} and λ_{Edd} of individual AGN.

A number of complications arise when measuring L_{bol} and M_{BH} from a large ($N > 100$) sample of galaxies. The majority of the total luminosity is emitted from the accretion disk in the extreme ultraviolet and ultraviolet energy bands (Shields 1978; Malkan & Sargent 1982; Mathews & Ferland 1987). While we used a fixed bolometric correction from the X-ray, this correction has been observed to vary depending on λ_{Edd} (Vasudevan et al. 2009) and L_{bol} (e.g., Just et al. 2007; Green et al. 2009). This issue deserves further study, though we would expect any biases to affect all line ratios whereas we find a much stronger correlation with [N II] $\lambda 6583/\text{H}\alpha$. Another complication is the use of separate methods of BH mass estimates. We note, however, that these two methods are tied to reproduce similar masses for systems where both are applicable (Graham et al. 2011; Woo et al. 2013), and that we find significant correlations for both type 1 and type 2 AGN, separately (Table 1). We will explore M_{BH} measurements for both types of AGN via different methods in a future study.

There are several possible physical mechanisms that might lead to the trends found between λ_{Edd} and emission line ratios such as [N II] $\lambda 6583/\text{H}\alpha$. Groves et al. (2006) and Stern & Laor (2013) found a dependence of emission-line diagnostics, particularly of the [N II] $\lambda 6583/\text{H}\alpha$, with host galaxy stellar mass. They postulated that this was a result of the mass metallicity relationship with more massive galaxies having more metals (Lequeux et al. 1979; Tremonti et al. 2004; Erb et al. 2006; Lee et al. 2006; Ellison et al. 2008; Maiolino et al. 2008; Mannucci et al. 2010; Lara-López et al. 2010). As more massive galaxies have more massive black holes, this follows the correlation found here with [N II] $\lambda 6583/\text{H}\alpha$ being positively correlated with M_{BH} and negatively correlated with L_{bol} . Stern & Laor (2013) showed that [O III] $\lambda 5007/\text{H}\beta$ mildly decreases with stellar mass since reduced [O III] $\lambda 5007$ emission is expected from higher metallicity and massive systems as [O III] $\lambda 5007$ is a main coolant and the temperature will be lower in massive systems. The less significant correlation between [O III] $\lambda 5007/\text{H}\beta$ and M_{BH} shown in Fig. 4 as compared to the [N II] $\lambda 6583/\text{H}\alpha$ which scales strongly with metallicity can be explained in this context. Another interesting possibility affecting this correlation could be from higher λ_{Edd} AGN have relatively weaker [O III] $\lambda 5007$ lines, as found by the ‘‘Eigenvector 1’’ relationships (e.g., Boroson & Green 1992).

A further possibility is that X-ray heating is inducing some of the negative correlation found between L_{bol} and the [N II] $\lambda 6583/\text{H}\alpha$ ratio. Ionizing ultraviolet photons produce a highly ionized zone on the illuminated face of the gas cloud while deeper in the cloud penetrating X-rays heat the gas and maintain an extended partially ionized region. Higher energy photons such as $\text{Ly}\alpha$ are destroyed by multiple scatterings ending in collisional excitation which enhances the Balmer lines (Weisheit et al. 1981; Krolik & Kallman 1983; Maloney et al. 1996). Strong X-rays (i.e., harder SEDs) that heat up hot electrons in partially ionized region also enhance collisional excitation of O^0 , N^+ , and S^+ . As a result, it is expected to see high [N II] $\lambda 6583/\text{H}\alpha$, [S II] $\lambda\lambda 6716, 6731/\text{H}\alpha$, and [O I] $\lambda 6300/\text{H}\alpha$.

Alternatively, the observed anti-correlation between emission line ratios ([N II] $\lambda 6583/\text{H}\alpha$ and [S II] $\lambda\lambda 6716, 6731/\text{H}\alpha$) and λ_{Edd} may be due to radiatively driven outflows in high λ_{Edd} systems. Radiatively accelerated wind is predicted to be proportional to λ_{Edd} (Shlosman et al. 1985; Arav et al. 1994; Murray et al. 1995; Hamann 1998; Proga et al. 2000; Chelouche & Netzer 2001). This is consistent with the observed blueshift of broad as well as narrow absorption lines (Misawa et al. 2007) often seen in quasars. In the context of a prevalent outflow in high λ_{Edd} AGN, the optical-UV SED of the accretion disk is expected to be softer when λ_{Edd} is $\gtrsim 0.3$ (King & Pounds 2003; Pounds et al. 2003; Reeves et al. 2003; Tombesi et al. 2010, 2011; Slone & Netzer 2012; Veilleux et al. 2016; Woo et al. 2016). As hot accreting gas is removed by ejecting outflows, the formation of collisionally excited emission lines is expected to be suppressed. It is important to note, however, that the anti-correlation between optical emission line ratio and λ_{Edd} is only appeared in [N II] $\lambda 6583/\text{H}\alpha$ and [S II] $\lambda\lambda 6716, 6731/\text{H}\alpha$ but not in other line ratios.

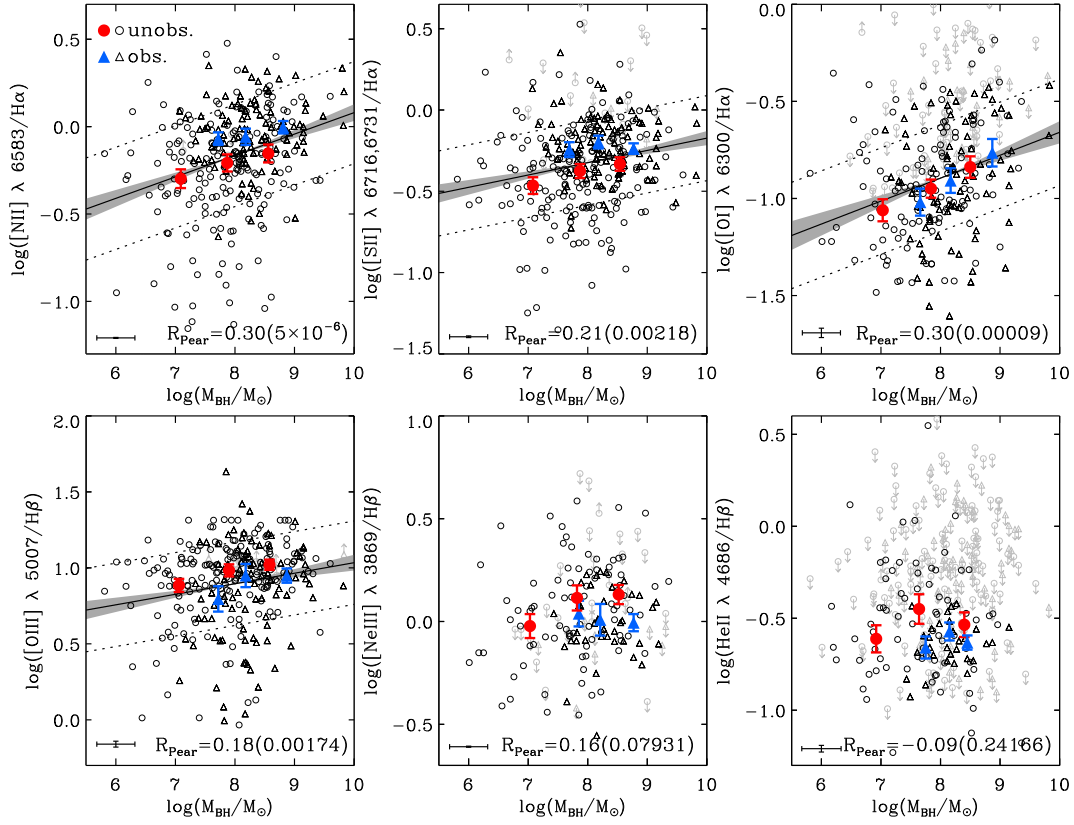


Figure 4. Optical emission line ratio versus black hole mass. The format is the same as that of Fig. 2

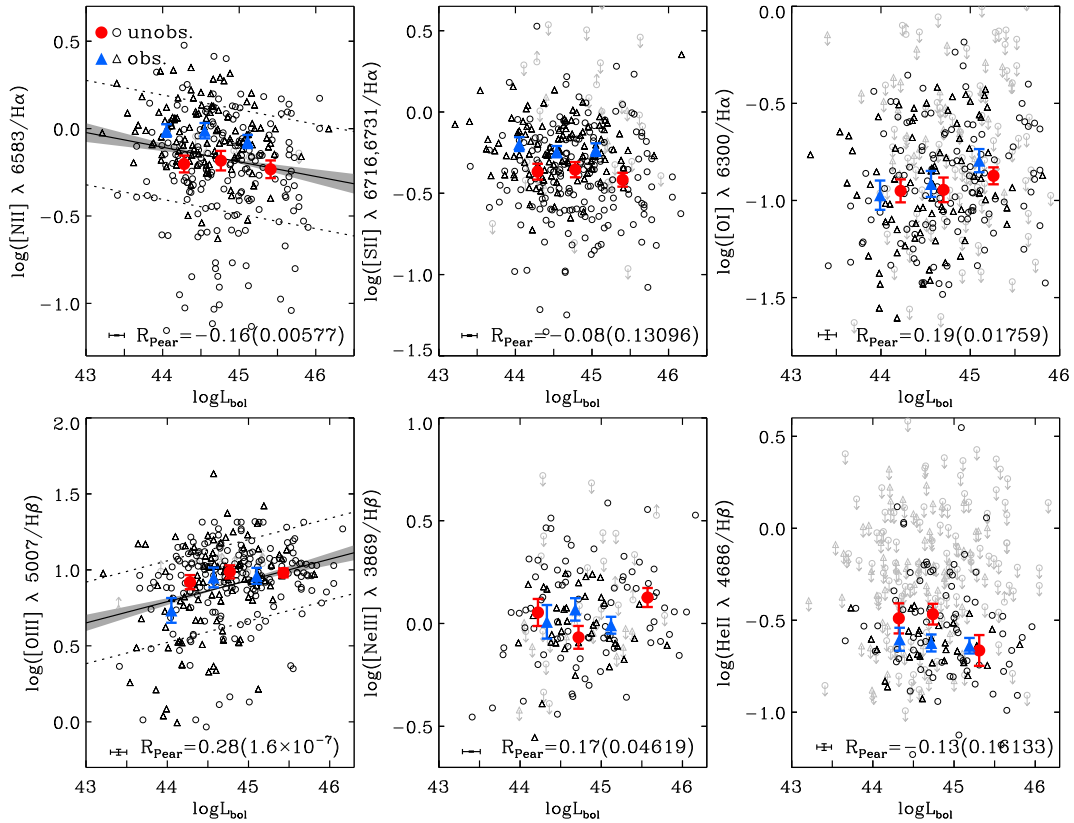


Figure 5. Optical emission line ratio versus bolometric luminosity. The format is the same as that of Fig. 2

5 SUMMARY

We present observed correlations between AGN Eddington ratio (λ_{Edd}), black hole mass (M_{BH}), and bolometric luminosity (L_{bol}) and narrow emission line ratios ([N II] $\lambda 6583/\text{H}\alpha$, [S II] $\lambda\lambda 6716, 6731/\text{H}\alpha$, [O I] $\lambda 6300/\text{H}\alpha$, [O III] $\lambda 5007/\text{H}\beta$, [Ne III] $\lambda 3869/\text{H}\beta$, and He II $\lambda 4686/\text{H}\beta$) for hard X-ray selected AGN from the BASS. The results of this study are:

- λ_{Edd} is anti-correlated with both the [N II] $\lambda 6583/\text{H}\alpha$ and [S II] $\lambda\lambda 6716, 6731/\text{H}\alpha$ ratios, but not with other line ratios.
- [N II] $\lambda 6583/\text{H}\alpha$ exhibits a significantly stronger anti-correlation with λ_{Edd} than [S II] $\lambda\lambda 6716, 6731/\text{H}\alpha$.
- The correlation shown in [N II] $\lambda 6583/\text{H}\alpha$ with M_{BH} is more significant than with L_{bol} .
- The correlation appeared in [N II] $\lambda 6583/\text{H}\alpha$ with M_{BH} might be a result of the mass metallicity relationship.
- The observed relationship between λ_{Edd} and [N II] $\lambda 6583/\text{H}\alpha$ ratio could be explained by considering X-ray heating processes and removal of material due to energetic outflow in the high λ_{Edd} state.
- The [N II] $\lambda 6583/\text{H}\alpha$ ratio could in principle be used to measure accretion efficiencies and black hole masses of high redshift obscured AGN (equation 2).

ACKNOWLEDGEMENTS

K.O. and K.S. acknowledge support from the Swiss National Science Foundation (SNSF) through Project grant 200021_157021. M. K. acknowledges support from the SNSF through the Ambizione fellowship grant PZ00P2_154799/1. M.K. and K. S. acknowledge support from SNFS Professorship grant PP00P2 138979/1. C.R. acknowledges financial support from the CONICYT-Chile “EMBIGGEN” Anillo (grant ACT1101), FONDECYT 1141218 and Basal-CATA PFB-06/2007. E.T. acknowledges support from the CONICYT-Chile “EMBIGGEN” Anillo (grant ACT1101), FONDECYT 1160999 and Basal-CATA PFB-06/2007. The work of DS was carried out at the Jet Propulsion Laboratory, California Institute of Technology, under a contract with NASA. This research has made use of NASA’s ADS Service.

Facilities: Swift, UH:2.2m, SDSS, KPNO:2.1m, FLWO:1.5m (FAST), Shane (Kast Double spectrograph), CTIO:1.5m, Hale, Gemini:South, Gemini:North, Radcliffe, Perkins

REFERENCES

Abazajian K. N., et al., 2009, *ApJS*, **182**, 543
 Alam S., et al., 2015, *ApJS*, **219**, 12
 Arav N., Li Z.-Y., Begelman M. C., 1994, *ApJ*, **432**, 62
 Baldwin J. A., Phillips M. M., Terlevich R., 1981, *PASP*, **93**, 5
 Barger A. J., Cowie L. L., Mushotzky R. F., Richards E. A., 2001, *AJ*, **121**, 662
 Barthelmy S. D., et al., 2005, *Space Sci. Rev.*, **120**, 143
 Baumgartner W. H., Tueller J., Markwardt C. B., Skinner G. K., Barthelmy S., Mushotzky R. F., Evans P. A., Gehrels N., 2013, *ApJS*, **207**, 19

Berney S., et al., 2015, *MNRAS*, **454**, 3622
 Boroson T. A., Green R. F., 1992, *ApJS*, **80**, 109
 Caccianiga A., Severgnini P., Della Ceca R., Maccacaro T., Carrera F. J., Page M. J., 2007, *A&A*, **470**, 557
 Campbell L. A., et al., 2014, *MNRAS*, **443**, 1231
 Cappellari M., Emsellem E., 2004, *PASP*, **116**, 138
 Chelouche D., Netzer H., 2001, *MNRAS*, **326**, 916
 Comastri A., et al., 2002, *ApJ*, **571**, 771
 Ellison S. L., Patton D. R., Simard L., McConnachie A. W., 2008, *ApJ*, **672**, L107
 Elvis M., Schreier E. J., Tonry J., Davis M., Huchra J. P., 1981, *ApJ*, **246**, 20
 Erb D. K., Shapley A. E., Pettini M., Steidel C. C., Reddy N. A., Adelberger K. L., 2006, *ApJ*, **644**, 813
 Gehrels N., et al., 2004, *ApJ*, **611**, 1005
 Graham A. W., Onken C. A., Athanassoula E., Combes F., 2011, *MNRAS*, **412**, 2211
 Green P. J., et al., 2009, *ApJ*, **690**, 644
 Greene J. E., Ho L. C., 2005, *ApJ*, **630**, 122
 Griffiths R. E., Georgantopoulos I., Boyle B. J., Stewart G. C., Shanks T., della Ceca R., 1995, *MNRAS*, **275**, 77
 Groves B. A., Heckman T. M., Kauffmann G., 2006, *MNRAS*, **371**, 1559
 Hamann F., 1998, *ApJ*, **500**, 798
 Harrison F. A., et al., 2013, *ApJ*, **770**, 103
 Iwasawa K., Koyama K., Awaki H., Kunieda H., Makishima K., Tsuru T., Ohashi T., Nakai N., 1993, *ApJ*, **409**, 155
 Jones D. H., et al., 2009, *MNRAS*, **399**, 683
 Just D. W., Brandt W. N., Shemmer O., Steffen A. T., Schneider D. P., Chartas G., Garmire G. P., 2007, *ApJ*, **665**, 1004
 Kauffmann G., et al., 2003, *MNRAS*, **346**, 1055
 Kelly B. C., 2007, *ApJ*, **665**, 1489
 Kewley L. J., Dopita M. A., Sutherland R. S., Heisler C. A., Trevena J., 2001, *ApJ*, **556**, 121
 Kewley L. J., Groves B., Kauffmann G., Heckman T., 2006, *MNRAS*, **372**, 961
 King A. R., Pounds K. A., 2003, *MNRAS*, **345**, 657
 Kormendy J., Ho L. C., 2013, *ARA&A*, **51**, 511
 Koss M. J., et al., 2016, *ApJ*, **825**, 85
 Krolik J. H., Kallman T. R., 1983, *ApJ*, **267**, 610
 Lara-López M. A., et al., 2010, *A&A*, **521**, L53
 Lee H., Skillman E. D., Cannon J. M., Jackson D. C., Gehrz R. D., Polomski E. F., Woodward C. E., 2006, *ApJ*, **647**, 970
 Lequeux J., Peimbert M., Rayo J. F., Serrano A., Torres-Peimbert S., 1979, *A&A*, **80**, 155
 Maiolino R., Salvati M., Bassani L., Dadina M., della Ceca R., Matt G., Risaliti G., Zamorani G., 1998, *A&A*, **338**, 781
 Maiolino R., et al., 2008, *A&A*, **488**, 463
 Malkan M. A., Sargent W. L. W., 1982, *ApJ*, **254**, 22
 Maloney P. R., Hollenbach D. J., Tielens A. G. G. M., 1996, *ApJ*, **466**, 561
 Mannucci F., Cresci G., Maiolino R., Marconi A., Gnerucci A., 2010, *MNRAS*, **408**, 2115
 Marconi A., Risaliti G., Gilli R., Hunt L. K., Maiolino R., Salvati M., 2004, *MNRAS*, **351**, 169
 Massaro E., Giommi P., Leto C., Marchegiani P., Maselli A., Perri M., Piranomonte S., Sclavi S., 2009, *A&A*, **495**, 691
 Mathews W. G., Ferland G. J., 1987, *ApJ*, **323**, 456
 Misawa T., Charlton J. C., Eracleous M., Ganguly R., Tytler D., Kirkman D., Suzuki N., Lubin D., 2007, *ApJS*, **171**, 1
 Murray N., Chiang J., Grossman S. A., Voit G. M., 1995, *ApJ*, **451**, 498
 Mushotzky R. F., Done C., Pounds K. A., 1993, *ARA&A*, **31**, 717
 Oh K., Sarzi M., Schawinski K., Yi S. K., 2011, *ApJS*, **195**, 13
 Oh K., Yi S. K., Schawinski K., Koss M., Trakhtenbrot B., Soto K., 2015, *ApJS*, **219**, 1
 Pounds K. A., King A. R., Page K. L., O’Brien P. T., 2003, *MNRAS*, **346**, 1025

- Proga D., Stone J. M., Kallman T. R., 2000, *ApJ*, **543**, 686
- Reeves J. N., O'Brien P. T., Ward M. J., 2003, *ApJ*, **593**, L65
- Reyes R., et al., 2008, *AJ*, **136**, 2373
- Ricci C., Ueda Y., Koss M. J., Trakhtenbrot B., Bauer F. E., Gandhi P., 2015, *ApJ*, **815**, L13
- Rigby J. R., Rieke G. H., Donley J. L., Alonso-Herrero A., Pérez-González P. G., 2006, *ApJ*, **645**, 115
- Rigby J. R., Diamond-Stanic A. M., Aniano G., 2009, *ApJ*, **700**, 1878
- Sarzi M., et al., 2006, *MNRAS*, **366**, 1151
- Schawinski K., Thomas D., Sarzi M., Maraston C., Kaviraj S., Joo S.-J., Yi S. K., Silk J., 2007, *MNRAS*, **382**, 1415
- Schawinski K., Koss M., Berney S., Sartori L. F., 2015, *MNRAS*, **451**, 2517
- Shields G. A., 1978, *Nature*, **272**, 706
- Shlosman I., Vitello P. A., Shaviv G., 1985, *ApJ*, **294**, 96
- Slone O., Netzer H., 2012, *MNRAS*, **426**, 656
- Stern J., Laor A., 2013, *MNRAS*, **431**, 836
- Tombesi F., Cappi M., Reeves J. N., Palumbo G. G. C., Yaqoob T., Braito V., Dadina M., 2010, *A&A*, **521**, A57
- Tombesi F., Cappi M., Reeves J. N., Palumbo G. G. C., Braito V., Dadina M., 2011, *ApJ*, **742**, 44
- Trakhtenbrot B., Netzer H., 2012, *MNRAS*, **427**, 3081
- Tremonti C. A., et al., 2004, *ApJ*, **613**, 898
- Vasudevan R. V., Mushotzky R. F., Winter L. M., Fabian A. C., 2009, *MNRAS*, **399**, 1553
- Veilleux S., Osterbrock D. E., 1987, *ApJS*, **63**, 295
- Veilleux S., Meléndez M., Tripp T. M., Hamann F., Rupke D. S. N., 2016, *ApJ*, **825**, 42
- Weisheit J. C., Tarter C. B., Shields G. A., 1981, *ApJ*, **245**, 406
- Winkler C., et al., 2003, *A&A*, **411**, L1
- Woo J.-H., Schulze A., Park D., Kang W.-R., Kim S. C., Riechers D. A., 2013, *ApJ*, **772**, 49
- Woo J.-H., Bae H.-J., Son D., Karouzos M., 2016, *ApJ*, **817**, 108
- Yuan S., Strauss M. A., Zakamska N. L., 2016, *MNRAS*, **462**, 1603

This paper has been typeset from a $\text{\TeX}/\text{\LaTeX}$ file prepared by the author.